System/Usage Impact of Operating the SLR2000 at 2 kHz*

Dr. Paul Titterton, Harold Sweeney and Donald Leonard
EOO, Inc., 269 N. Mathilda Ave, Sunnyvale, CA 94086-4830
(408) 738-5390;FAX: (408) 738-5399; e-mail: EOOINC@AOL.COM

* Supported by AlliedSignal Technical Services Corp. and NASA Goddard Space Flight Center

Overview

The SLR2000 has been discussed at two previous workshops as well as in other references cited in the bibliography. This paper discusses the implications of operating at the relatively high Pulse Repetition Frequency (PRF) of 2 kHz. The aspects discussed include:

- Impact of Eyesafe and Affordable Operation
- Signal Level and Detection by Time Correlation of Counts
- Corresponding Noise Count Rejection Approach
- Number of Pulses Simultaneously in Flight
- Backscatter from the Common Optics and Atmosphere
- Receiver Blanking Times
- Pro-Active Pulse Repetition Interval Control to Avoid Signal Blanking

Impact of Eyesafe and Affordable Operation

In order for a system operating in the green to be both eyesafe at the aperture and operate inexpensively , the design employs common transmit/receive optics. In a normal system, the transmitter aperture would be far smaller than the receiver --- but eye safety, using the ANSI standards for short pulses in the green, results in the relationship between energy per pulse and PRF in Equation 1, and evaluated in Table 1 and Figure 1, given for a 40 cm common transmit/receive aperture, selected for affordabilty.

$$\mathbf{E_p = 888.6\,[PRF]^{-1/4}}\ \mu\text{joules} \qquad (1)$$

Table 1 /Figure 1. Green Eyesafe Energy per pulse vs Laser PRF for 40 cm aperture

PRF (Hz)	Energy/Pulse (µjoules)
2000	132.8
1900	134.5
1800	136.4
1700	138.4
1600	140.5
1500	142.8
1000	158.0

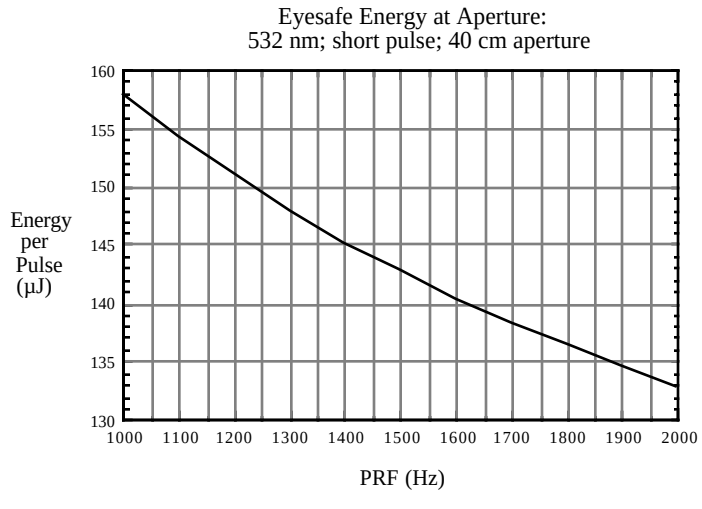

Signal Level and Detection by Time Correlation of Counts

This 40 cm aperture and 2 kHz PRF green system is then the basis of further analysis. The complete hardware parameters for the analyzed system are listed in Table 2.

Table 2. SLR 2000 Hardware Parameters

Transmitter Side	Receiver Side
Wavelength: 532 nm	Filter Bandpass : 1.2 Å (50% throughput) [B_{opt}]
Energy Per Pulse: 133 μjoule [$E_p\gamma_t$]	Effective Quantum Efficiency: 12 % [η]
Pulse Repetition Frequency: 2000 Hz	Total Dark Counts: < 10^4 /second @ 20 °C
Pulsewidth: 140 psec	Resolution: < 100 psec
Transmitter Aperture: 40 cm diam. [D_t]	Receiver Aperture: 40 cm diam. [D_r]
Optical Transmission: > 80 % [γ_t]	Optical Transmission: > 30 % [γ_r]
Half Angle Beamwidth: 20 mrad [θ_t]	Half Angle Beamwidth: 25 μrad [θ_r]
Irradiance Distribution - At Aperture: Top Hat - Far Field: Airy Disc	Field-of-View : Sharp Edged Uniform Sensitivity
Pointing Jitter: < 5 μradians (nominal)	Boresight with Transmitter: < 5 μradians
Pointing Offset: < 5 μradians (nominal)	Special: Quadrant Detector

Given these parameters, we have estimated the limiting (lowest) signal levels per pulse in Table 3 for representative low, medium and high altitude satellites at the lowest elevation angles. In all cases the signal level is estimated in terms of the mean signal photo-electrons (pe's) at the cathode per pulse, n^s_{pe}, which is << 1. At a PRF of 2 kHz, Starlette will return 18 pe per second, while the other two will return only an average of 0.6 pe per second.

Table 3. Limiting Signal Levels during Low Angle Acquisition

Satellite Target	Elevation Angle	n^s_{pe}
Starlette	20°	0.009
LAGEOS	20°	0.0003
ETALON (GPS)	~ 30°	0.0003

To acquire the satellite at these levels, we employ correlation-aided detection. We define:

Frame = # of range gates used in signal detection;
Range Gate = T_{rg}, time interval within which the signal pulse will occur;
Bin Width = t_{bin}, time interval in which multiple signal photons will occur (i.e. will be correlated in arrival time), given the predictive and system timing uncertainties,

For Poisson Statistics, the probability that $\geq$ k signal photo-electrons will be detected in a single (corresponding) bin, after a mean number of N^s_{pe} signal photo-electrons have been detected, is

$$P_D(\geq k) = 1 - e^{-N_{pe}^s}\left(\sum_{j=0}^{k-1}\frac{\left(N_{pe}^s\right)^j}{j!}\right). \qquad (2)$$

Using $N_{pe}^s = 10$ and a correlation parameter (k) of 6 as a detection criterion, the single frame Probability of Detection is 93%.

Noise Count Rejection Approach: For the clear daytime sky, the total noise count rate is $\dot{n}_{pe}^n = 5.2(10^4)$ (sec^{-1}), neglecting signal backscatter (discussed later in this paper).

The number of bins per range gate is

$$n_{bin} = \frac{T_{rg}}{0.5\ nsec},\ for\ \Delta\dot{R}\left(\frac{N_{pe}^s}{n_{pe}^s}\right)\left(\frac{\Delta t_{bias}}{2000}\right) < 0.5\ nsec; \qquad (3)$$

for $\Delta\dot{R} = $ Range Rate Uncertainty; $\Delta t_{bias} = $ Total Time Bias.

The mean number of noise counts per bin over the frame is

$$\overline{m} = 5\left(10^{-10}\right)\frac{\dot{n}_{pe}^n\left(N_{pe}^s\right)}{\left(n_{pe}^s\right)},\ for\ t_{bin} = 0.5\ nsec. \qquad (4)$$

The False Acquisition Probability itself is given by Equation 5 and evaluated in Figure 2.

$$P_{FalseAcq} = 1 - e^{-n_{bin}\left\{\overline{m} - \ln\left[\sum_{j=0}^{k-1}\frac{\overline{m}^j}{j!}\right]\right\}}. \qquad (5)$$

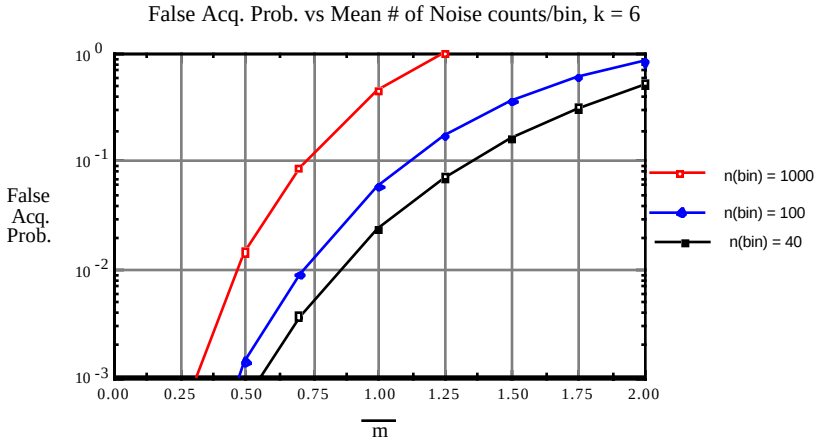

Figure 2. Caption Above.

N of M Acquisition Technique: In some cases, this single frame correlation technique does not work, i.e. there is insufficient signal to provide a detection probability per frame which is > 90% and a false acquisition per frame which is ≤ 1%. In this case, one views M frames, each with a signal detection probability of < 90%. Success is declared if in N of the M frames the signal is detected, and one can achieve an overall detection probability of > 90% et al.

The detection and false acquisition probabilities for this approach are given by

$$P_D^{NofM} = \sum_{i=N}^{M} \frac{M!}{(M-i)!\,i!} \left(P_D^{fr}\right)^i \left(1 - P_D^{fr}\right)^{M-i} \qquad (6)$$

and

$$P_{FalseAcq}^{NofM} = \sum_{i=N}^{M} \frac{M!}{(M-i)!\,i!} \left(P_{FalseAcq}^{fr}\right)^i \left(1 - P_{FalseAcq}^{fr}\right)^{M-i} \qquad (7)$$

The probabilities with the superscript "fr" (= frame) are those previously calculated for the single frame acquisition analysis, i.e. Equations 2 and 5.

Correlation-Aided Detection, with either the single frame or N of M approach, provides full performance against the noise generated by background and dark counts, for all satellite targets.

Number of Pulses Simultaneously in Flight @ 2 kHz PRF

Because of the high PRF, there are very many pulses simultaneously in flight. The $\#\text{ in Flight} = \frac{2\,(\text{Range})\,\text{PRF}}{(\text{Speed of Light})}$, and is evaluated for Starlette, LAGEOS and ETALON in Table 4 and Figure 3, as a function of elevation angle.

Table 4 / Figure 3. # of Pulses in Flight

Elev. Angle	Starlette	LAGEOS	ETALON
20°	27.4	113.7	302.6
30°	21.9	103.6	290.6
40°	18.3	95.5	280.3
50°	16.0	89.1	271.6
60°	14.5	84.4	264.9
70°	13.5	81.2	260.0
80°	12.9	79.22	257.1
90°	12.8	78.72	256.2

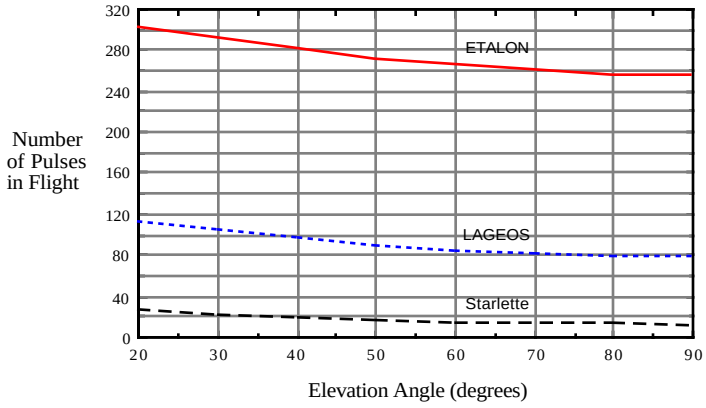

Backscatter from the Common Optics

Because of the large number of pulses in flight and the extremely low signal levels, we must account for all sources of backscattered photons. The first source of such a noise signal is the common receive-transmit optics. In order to detect the infrequent signal pe's, any photons scattered out of the 10^{14} transmitted must be prevented from reaching the detector. The practical way to provide such isolation is to turn the detector off (blank it) during transmitter firing, and arrange the system such that no signal pulses will return at that blanked time.

Backscatter from the Atmosphere

The atmosphere is common to both the transmitter beam and the receiver field-of-view over much of the path. Backscatter from the atmosphere would mask the returned signal photons that occur during the time that the backscatter is too large.

We estimate that the number of backscatter-generated pe's in a 100 nsec range gate is

$$n_{pe}^{bsc/rg} = 2.414\left(10^{13}\right)\rho\sigma(\pi)\frac{\tau_p^2}{R^2}\gamma_{obs}, \qquad \text{100 nsec range gate.} \qquad (8)$$

for ρ = number density of the scattering particles, assumed to be molecules for the higher altitudes of interest; the model in the US Standard Atmosphere, 1962 is used here;
$\sigma(p)$ = backscatter cross-section of an individual particle --- for the molecular particles assumed here, we use $\sigma(p) = 7.08(10^{-28})$ cm^2/srad.
γ_{obs} = beam overlap factor, depends on the satellite and pointing strategy employed, through the three parameters:

θ_t = Half-angle transmitter beam divergence = 20 μradians for all cases ;
θ_r = Half-angle receiver field-of-view = 25 μradians for all the cases ;
θ_{OS} = Angular offset between the transmitter beam and the receiver field of view, measured between their respective axes.

Beam-FOV Overlap Factor : The beams are offset to compensate for the point-ahead/point-behind for the line-of-sight to the satellite, as estimated in Figure 4 for the three satellite targets.

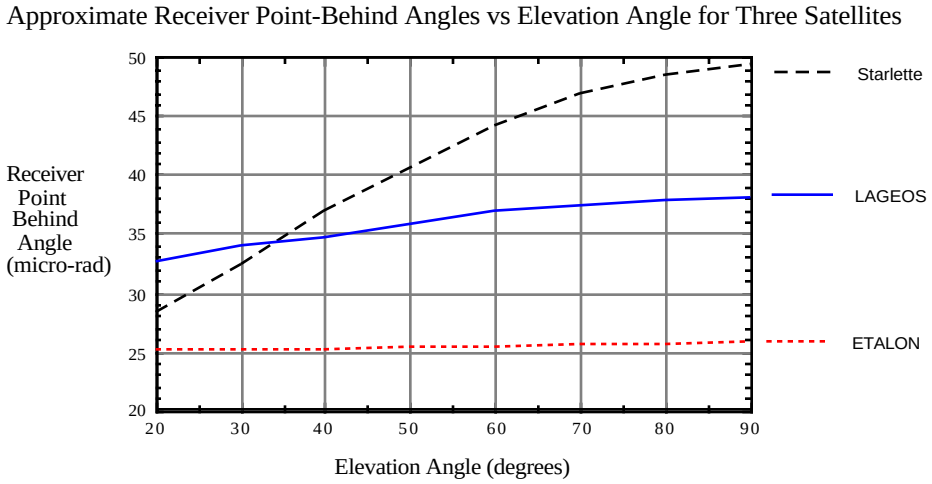

Figure 4. Caption Above.

We take the limiting values to be: Starlette, 20° : 28 μradians;
LAGEOS, 20°: 33 μradians;
ETALON, 30°: 25 μradians.

Using a simple geometric analysis, we then estimate that the overlap factor for LAGEOS and ETALON in the far field are given by: γ_{obs} = 0.2, LAGEOS and 0.4, ETALON.

We can then estimate the backscattering strength as a function of range for LAGEOS, as shown in Table 5 and Figure 5.

Table 5/Figure 5. Estimated Backscatter pe per range gate for LAGEOS at 20° elevation

H(km)	R(km)	$n_{pe}^{bsc/rg}$
2	5.84	0.106
4	11.67	0.0212
6	17.48	0.00766
8	23.3	0.00342
10	29.11	0.00194
12	34.84	0.00093
14	40.6	0.00050
15	43.5	0.00041
16	46.34	0.00028
17.5	50.67	0.000205
20	57.8	0.000105

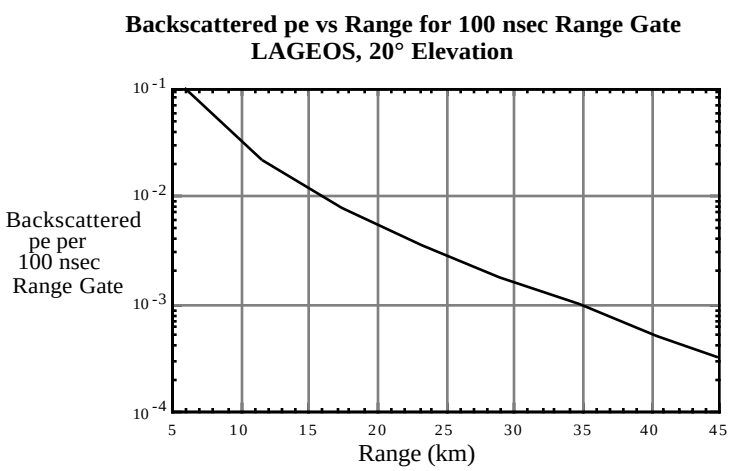

Receiver Blanking Times

We now estimate the required receiver blanking time:

Common Optical Path: Turn Receiver off while the laser is firing; jitter in the laser firing time is taken to be about ~ ± 20 μseconds, so allocate 40 μseconds, with the nominal laser firing time occurring 20 μseconds after the start of this blanking time.

Atmospheric Backscattering: Time after nominal fire time during which the atmospheric backscatter will cause a high false acquisition probability.

Net Blanking Time: $T_B(\text{total}) = T_B(\text{Atmospheric}) + 40$ μseconds.

Blanking Time Estimation Methodology

Based on the above analysis and considerations, we have derived the following methodology for estimating the blanking time required in a given situation:

1. Calculate the time to acquire for the acquisition technique used, single frame or N/M.
2. Estimate the value of the mean noise counts per bin, $\overline{m}$, for the nominal background and dark noise counts, from Equation 4, using $\dot{n}_{pe}^{n}$ = 52,000 noise counts/second; N_{pe}^{s} = 10, providing a 93% detection probability for a correlation parameter k = 6; n_{pe}^{s} = value appropriate to the satellite target at the elevation angle of interest.
3. Calculate the probability of false acquisition for the acquisition technique considered. For the single frame technique, the appropriate expression is Equation 5;
where n_{bin} = number of 500 pico-second range bins within the range gate.
4. If the derived false acquisition probability is ~ 1%, or can be increased somewhat above this value without materially degrading system performance, estimate the allowable (larger) value of $\overline{m}$ that will correspond to the selected/new value of $P_{FalseAcq}$.
5. From Equation 4, calculate the allowable additional noise count rate for this increased value of $\overline{m}$.
6. Allocate this added noise count rate to atmospheric backscatter, multiply the allowable rate by the range gate width, and determine at what range the backscatter per range gate falls below the allowed value. (In our earlier analysis the range gate was assumed to be 100 nsec. For other gate widths those results can be scaled.)
7. Convert this atmospheric backscatter range to the two way time of flight, and this is the atmospheric blanking time.
8. Add 40 μseconds to this result, yielding the total backscatter value.

For the 2 kHz PRF, the Pulse Repetition Interval (PRI) is 500 μseconds. For some conditions, the blanking time calculated from the above procedure can be a substantial fraction of this value. If, for example, the blanking time is 200 μseconds, a simple blanking of the receiver would remove 40% (200 ÷ 500) of the return pulses from consideration, leading an extended acquisition time, or even making realistic acquisition impractical. Because this blanking time is calculable, and the relative positions of the pulses in their flight to/from the target are predictable, we have devised a technique that enables the use of all signal pulses, nearly independent of the relative size of the blanking time. This is discussed next.

Pro-Active PRI Control to Avoid Signal Blanking Control (to avoid signal blanking)
Single Pulse in Flight: We define the following parameters in Figure 6:

T_B = blanking time;

T_{fl} = two way time of flight from the transceiver to the target; $T_{fl} = \frac{2R_{t\,arg}}{c}$,

for R_{targ} = range to the satellite target from the transceiver, c = speed of light;

T_c = clear time, during which the receiver can usefully receive signal pulses.

T_o = Pulse Repetition interval (PRI).

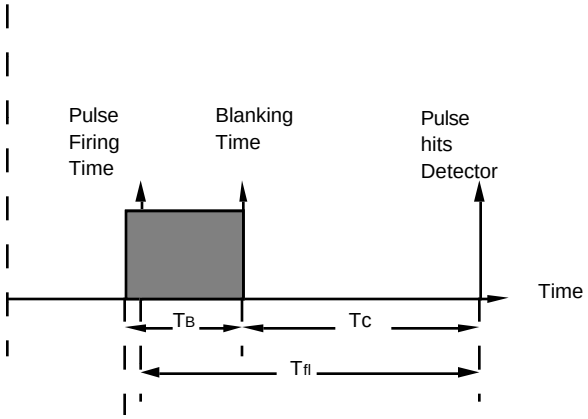

Figure 6. Definition of blanking time and PRI control Parameters.

*This time includes the laser jitter firing time, and depends on signal strength, i.e. the blanking time is that time over which the backscatter-generated (and therefore effectively noise) pe's will significantly degrade system performance. For large signal levels, the allowable backscatter is much larger than for small signal returns.

For a single pulse in flight, the equations for the clear and blanked times are shown in Table 6.

Table 6. Single pulse-in-flight blanking and clear conditions equations

Blanked	Clear
$T_{fl} < T_B$, or, $\frac{2R_{targ}}{c} < T_B$, or, $R_{targ} < \frac{cT_B}{2}$	$T_B < T_{fl}$, or, $T_B < \frac{2R_{targ}}{c}$, or, $\frac{cT_B}{2} < R_{targ}$

k pulses in Flight: When there are k pulses in flight at any one time, blanked times will exist from (kT_o) to $(kT_o + T_B)$, i.e. each of the k pulses carries its associated blanking time. However, because the target range (or time of flight) is known approximately, we can pre-determine whether or not the target can be detected, from the point of view of receiver blanking. For example, the target can be detected if

$$(kT_o + T_B) \le T_{fl} \le (k+1)T_o \qquad (9)$$

since kT_0+T_B is the end of one blanking time, and $(k+1)T_0$ the beginning of the next one. This is further defined in Table 7.

Table 7. k pulses in flight, blanking and clear conditions

Blanked	Clear
$T_{fl} < T_B$; $kT_o \le T_{fl} \le kT_o + T_B$, or $R_{targ} < \frac{cT_B}{2}$; $\frac{ckT_o}{2} \le R_{targ} \le \frac{c(kT_o + T_B)}{2}$	$kT_o + T_B \le T_{fl} \le (k+1)T_o$, or $\frac{c(kT_o + T_B)}{2} \le R_{targ} \le \frac{c(k+1)T_o}{2}$

From this table, it is evident that some pulses will be blanked as the range changes. If the blanking time is very short compared to the inter-pulse interval, these blanked pulses may constitute an acceptable loss of pulse returns; In general, however, one should not waste pulses in a signal starved system, e.g. during acquisition, and so we consider changing the only parameter over which we have control --- the Pulse Repetition Interval (PRI).

Deriving PRI Values

Given a nominal pulse repetition interval T_o and a required receiver blanking duration of T_B, along with the minimum and maximum ranges to the target, the number of alternate PRI's and the necessary PRI shift to avoid the loss of signal pulses can be determined.

Two PRI Values: Consider one alternate PRI, called T_1, in addition to the nominal T_o, such that

$$T_1 = T_o + \delta T. \qquad (10)$$

A range segment that is visible while operating with PRI = T_o extends from $(kT_o + T_B)$ to $(k+1)T_o$, and a corresponding range element visible with PRI = T_1 extends from $(kT_1 + T_B)$ to $(k+1)T_1$.

To attain continuous coverage (as shown in Figure 7)

$$(kT_o + T_B) \le kT_1 \quad \text{and} \quad (kT_1 + T_B) \le (k+1)T_o \qquad (11\ a,\ b)$$

which are the conditions that the blanking times for the two PRIs do not overlap.

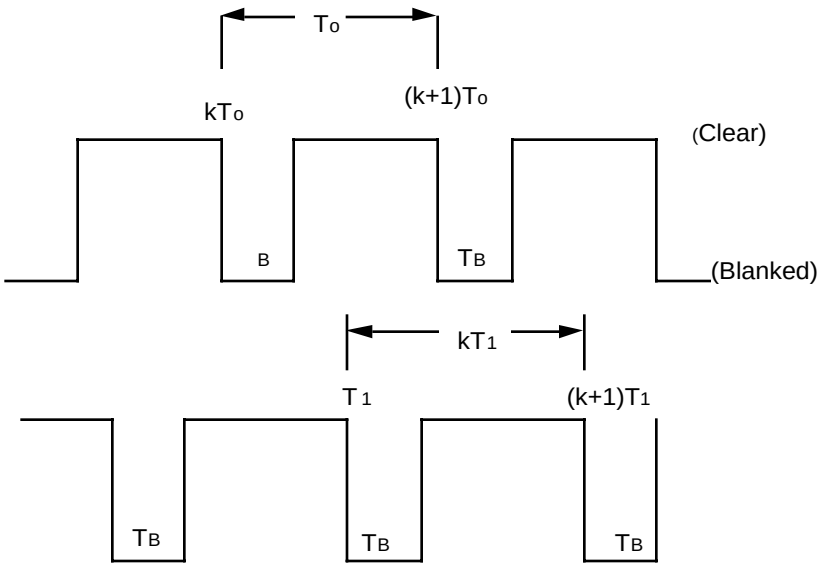

Figure 7. Timing of Interleaved Ranges: Two PRI Values

Substituting $T_1 = T_o + \delta T$,

$$(k+1)T_o + T_B \le (k+1)(T_o + \delta T) \Rightarrow T_B \le k\,\delta T,$$
$$k(T_o + \delta T) + T_B \le (k+1)T_o \Rightarrow k\,\delta T + T_B \le T_0 \qquad \text{which imply } \frac{T_B}{k} \le \delta T \le \frac{T_o - T_B}{k}.$$

The strictest condition (so it holds for all values of k) is

$$\frac{T_B}{k_{min}} \le \delta T \le \frac{T_o - T_B}{k_{max}}, \tag{12}$$

condition if only two PRI values, T_O and T_O +dT, are to be used.

Three PRI Values: We consider the PRI values: T_o, $T_1 = T_o + \delta T$, and $T_2 = T_o + 2\delta T$. Now three conditions must be satisfied, as seen in Figure 8:

$$kT_1 + T_B \le (k+1)T_0; \quad kT_2 + T_B \le (k+1)T_1; \quad kT_o + T_B \le kT_2$$

These equations state that the three blanking times must not fully overlap ---- so that for every time of flight there will be a selectable PRI which will provide clear conditions. Indeed, there are two values of the PRI which are clear for the equations and PRI's cited.

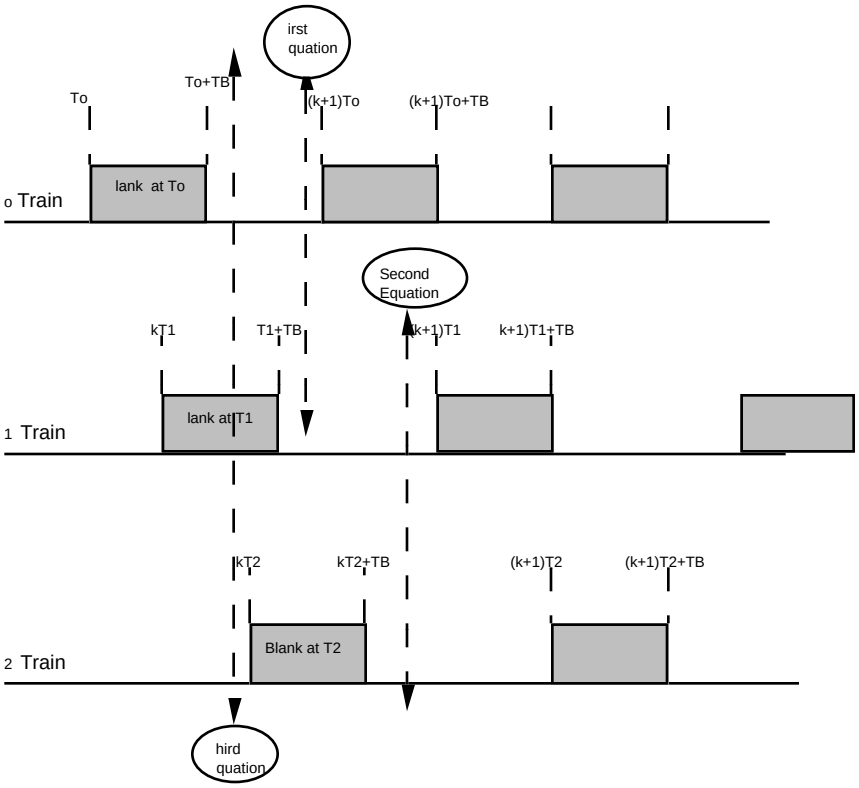

Figure 8. Three PRI clear path conditions.

The condition on δT for using just 3 PRIs is $\frac{T_B}{2k_{min}} \le \delta T \le \frac{T_o - T_B}{k_{max}}$ (13).

General Expression for Required Number of PRIs: We generalize an expression for the number "n" of PRI's that would be adequate

$$\frac{T_B}{(n-1)k_{min}} \le \delta T \le \frac{T_o - T_B}{k_{max}}, \qquad (14)$$

which can be further manipulated to provide an expression for the number of PRIs required:

$$n \ge \left(\frac{T_B}{T_o - T_b}\right)\frac{k_{max}}{k_{min}} + 1 \qquad (15)$$

Continuous PRI Variation: An alternate approach is to continuously vary the PRI, while keeping the number of pulses in transmit a constant. This approach has the advantageous feature that the detection time can be maintained at a fixed point just prior to the laser firing time. This is very desirable if the atmospheric backscatter is very severe close to the target, as for example the target being ranged is actually within the atmosphere rather than a satellite. For SLR2000, a finite set of PRIs was selected to optimize laser affordability.

Methodology of Quick Look Usage of T_B(total)

The pro-active PRI approach for full usage of all signal pulses follows the technique: For Single Frame Acquisition.

a. For the candidate S/C, determine the number of PRI's required: n;
b. Determine the reasonable PRI offset: δT;
c. If n = 2 and dT > 1 msec, adopt these values of n and δT as practical;
d. If n > 2 or δT< 1 msec, assess the hardware/software practicality of implementing the technique. If insuperable difficulties arise, go to N of M acquisition.

Examples: As an example, we have considered LAGEOS acquisition for the four conditions in Table 8. For these four cases, although substantial blanking times arise, 2 or 3 programmable values of the PRI will provide full orbital coverage, while missing no signal pulses.

Table 8. Blanking Times and PRI Parameters for the Four Cases
(adding 40 μsec for laser jitter)

Case #	n_{pe}^{s}	$\overline{m}$	Limiting Value of Backscattered pe/range gate	Corresponding molecular backscatter range (km)	Atmospheric Blanking Time (μ-sec)	Total Blanking Time (μ-sec)	Required # of PRIs	PRI Offset (μsec) δT
1	0.0003	0.9	0.00156	30.4	203	243	3	2
2	0.0003	0.99	0.0023	27.3	182	222	3	2.2
3	0.0004	0.9	0.0038	22.6	151	191	2	2.5
4	0.0004	0.99	0.0048	21.3	142	182	2	2.6

Acknowledgment

The authors acknowledge the many technical discussions with John Degnan and Jan McGarry of NASA Goddard Space Flight Center that have helped to guide the direction of this work, along with the support of Bud Donovan of AlliedSignal Technical Services Corporation. This work was sponsored by NASA Goddard through Purchase Orders No. HQ302756 and HQ307309.

Bibliography

J. J. Degnan, Millimeter Accuracy Satellite Laser Ranging: A Review, Geodynamics Series Volume 25, Contributions of Space Geodesy to Geodynamics: Technology, 1993.

J.J. Degnan, "SLR 2000" in "Satellite Laser Ranging in the 1990's", Proceedings of the Belmont Workshop, Elkridge, MD, NASA Conference Publication 3283, Ed. J.J. Degnan, pp. 101-106, February 1-2, 1994.

J.J. Degnan, SLR 2000: An Autonomous and Eyesafe Satellite Laser Ranging System, Ninth International Workshop on Laser Ranging Instrumentation, Canberra 1994, J. McK. Luck Ed., Volume 1, pps. 312-323.

J.F. McGarry, B. Conklin, W. Bane, R. Eichlinger, P. Seery and R.L. Ricketts, Tracking Satellites with the Totally Automated SLR2000 System, Ninth International Workshop on Laser Ranging Instrumentation, Canberra 1994, J. McK. Luck Ed., Volume 2, pps. 717-725.

P. Titterton and H. Sweeney, SLR 2000 Design and Processing Approach Sensitivity, EOO Report 94-003, Dec. 15, 1994. GSFC PO# S-44974-Z.

P. Titterton, H. Sweeney and T. Driscoll, SLR 2000 Analytical Study of 1060 nm Aided Acquisition and Tracking, EOO Report 95-007, Nov. 1, 1995, GSFC PO# S-61158-Z.

J.F. McGarry, J.J. Degnan, P.J. Titterton, H.E. Sweeney, B.P. Conklin and P.J. Dunn, Automated tracking for advanced satellite laser ranging systems, Paper 2739-08 in Acquisition, Tracking and Pointing X, Proceeding of the SPIE Volume 2739, M.K, Mastern and L.A. Stockum Editors, 10-11 Apr. 1996, pps. 89-103.

J. J. Degnan, J.F. McGarry, T. Zagwodski, P. Titterton, H. Sweeney, H. Donovan, M. Perry, B. Conklin, W. Decker, J. Cheek, T. Mallama and R. Rickleffs, An inexpensive, fully automated, eyesafe satellite laser ranging system, Tenth International Workshop on Laser Ranging, Shanghai, 1996,

J. McGarry, SLR2000 performance simulations, Tenth International Workshop on Laser Ranging, Shanghai, 1996,

P. Titterton and H. Sweeney, Correlation Processing Approach for Eyesafe SLR2000, Tenth International Workshop on Laser Ranging, Shanghai, 1996,

P. Titterton, H. Sweeney and T. Driscoll, ATSC SLR2000: Acquisition Algorithm Assessments (DRAFT), EOO Report 97-010, August 1997.

J.J. Degnan, SLR2000 Project: Engineering Overview and Status, Eleventh International Workshop on Laser Ranging, Deggendorf 1998.

J.J. Degnan and J.J. Zayhowski, SLR2000 Microlaser Performance: Theory vs Experiment, Eleventh International Workshop on Laser Ranging, Deggendorf 1998.

J. McGarry, J. Cheek, A. Mallama, N. Ton, B. Conklin, A. Mann, M. Sadeghighassami, M. Perry and R.L. Ricketts, SLR2000 Automated System Control Software.